university of groningen / faculty of science and engineering / artificial intelligence

Translating EEG-Derived Features into fMRI Signal Representations for Neuroimaging

Bachelor's Project Thesis

David Setoain, s4621255, d.s.setoain@student.rug.nl
Supervisors: Lisa Vortmann & Sönke Steffen

1 Abstract

Simultaneous EEG-fMRI has gained increasing attention due to their complementary strengths: EEG provides high temporal resolution, while fMRI offers accurate spatial resolution. Despite these advantages, integrating the two modalities poses challenges, including high noise levels and the elevated cost and limited accessibility of fMRI. This thesis addresses a gap in multimodal neuroimaging by investigating the feasibility of predicting fMRI signals directly from EEG data using an encoder-decoder model trained on simultaneous EEG-fMRI recordings. EEG features, including band power, peak frequency, aperiodic 1/f slope, burst dynamics, phase-locking value (PLV), amplitude-envelope correlation (AEC), and global field power (GFP) serve as inputs to predict fMRI activity. The study evaluates which EEG-derived features most effectively capture the spatial patterns typically observed in fMRI data. Although fully reconstructing an fMRI signal from EEG remains a complex challenge, several features demonstrate predictive potential, such as the maximum, minimum, and average amplitude per frequency band. These findings indicate that EEG contains latent spatial information that may approximate fMRI activity, suggesting that a reliable translation could be achieved with further modeling and research. By exploring this relationship, the thesis provides a foundation for computationally cheaper, temporally precise, and accessible brain mapping, with potential applications in both neuroscience research and clinical neuroimaging.

2 Introduction

2.1 Background and Context

In neuroscience, comprehending the human brain remains a major challenge due to its complexity. Understanding brain activity is crucial not only for clinical purposes but also for advancing cognitive science, developing brain-computer interfaces, and the study of functions such as memory, attention, and decision-making. Two widely used techniques, Electroencephalography (EEG) and Functional Magnetic Resonance Imaging (fMRI) have significantly contributed to this research, each offering distinct advantages.

EEG provides high temporal resolution, capturing fast neural oscillations by measuring the brain's electrical activity, but lacks spatial precision. On the other hand, fMRI offers high spatial resolution by measuring the blood-oxygen-level-dependent (BOLD) response, therefore localizing neural activity precisely even in deep cortical structures; however, fMRI has poor temporal resolution (Misulis & Abou-Khalil, 2013; Ulmer & Jansen, 2020). Ultimately, the advantages and disadvantages of these two modalities are reversed.

Despite their capability to compensate for each other's limitations when combined, their simultaneous use is uncommon. Mainly as a result of the technical and computational challenges involved in combining these techniques. Nevertheless, recent studies such as Warbrick (2022) have shown a growing interest in integrating the spatial and temporal advantages of both methods. Therefore, developing models capable of predicting or translating fMRI signals from EEG data alone can be a promising advancement in cognitive neuroscience. Such a model could ultimately enable more efficient and accessible neuroimaging.

2.2 Problem Statement and Motivation

While fMRI offers high spatial precision, its use is limited by high costs, low accessibility, and poor temporal resolution as a result of the inherent delay of the BOLD response. In contrast, EEG is more affordable and capable of measuring fast neural activity in the brain, making it ideal for continuous and real-time monitoring. Although many researchers such as Warbrick (2022) incorporate the strengths of both methods through simultaneous EEG-fMRI recordings, an alternative approach involves developing methods to translate EEG signals into spatially detailed representations similar to those produced by fMRI. This would offer a more practical solution for efficient brain monitoring in both cognitive research and clinical diagnosis.

Such models could enable spatially accurate brain monitoring using EEG alone, combining the powerful temporal resolution and practicality with the spatial precision of fMRI. This approach is particularly valuable in environments with limited access to MRI scanners or where real-time tracking is essential, for example, in intensive care units, neurodiagnostics, and brain-computer interface development. Furthermore, it opens new possibilities for advancing neuroimaging, cognitive research, and mobile diagnostics that can aid in resource-limited environments, supporting applications like epilepsy monitoring or sleep studies where traditional neuroimaging could be impractical. At the same time, this approach also contributes in achieving a deeper understanding of how electrophysiological signals measured by EEG relate to hemodynamic responses captured by fMRI. However, this method remains unexplored, and the EEG features that could potentially translate to fMRI signal representations are unclear.

2.3 Research Objectives

The primary objective of this thesis is to investigate the extent to which features derived from EEG recordings can be used to predict characteristics typically observed in fMRI signals. Specifically, the research aims to discover which features extracted from EEG data can predict spatial patterns observed in BOLD responses.

To achieve this objective, the study will:

- Extract a range of EEG features from a dataset involving simultaneous EEG-fMRI recordings during resting state.
- Develop and implement a translation model capable of mapping these EEG-derived features onto fMRI signal representations
- Evaluate the predictive accuracy of the model using statistical correlation metrics.
- Identify the EEG-derived features that most significantly contribute to accurate fMRI predictions, therefore bridging the gap between electrophysiological and hemodynamic brain signals.

By addressing these objectives, this study aims to contribute to the broader goal of enabling EEG approximations of fMRI data. A technique that can become crucial in both clinical research and diagnosis.

3 Theoretical Framework

3.1 Overview of EEG

Electroencephalography (EEG) is a widely used noninvasive medical test to record the brain's electrical activity through electrodes placed on the scalp. These electrodes detect voltage fluctuations caused by postsynaptic potentials resulting from neuronal populations, mainly in the cerebral cortex (Misulis & Abou-Khalil, 2013).

The main advantage of EEG lies in its accurate temporal resolution, as stated earlier, allowing it to capture neural events with millisecond precision. This makes it particularly valuable for studying fast-changing brain processes such as attention, memory encoding, and decision-making.

However, EEG has some limitations, such as its low spatial resolution. This is due to the inverse problem, which is the challenge that many different possible configurations of neural sources inside the brain can produce the same voltage pattern measured on the scalp. Additionally, electrical signals can get distorted as they pass through the skull or scalp, making the localization of EEG activity imprecise (Im, 2018). As a result, the accuracy in source localization for EEG is limited to 2-3 centimeters in general, and for deeper brain regions,

several centimeters or often not detectable at all. EEG is most sensitive to cortical activity near the surface of the brain, while its ability to detect signals from deep brain regions is limited due to the proximity of the sensors to the brain regions increasing as the electrodes are placed on the scalp.

Despite these limitations, EEG is still indispensable for cognitive neuroscience and clinical diagnosis (Budzynski, 2009). It is routinely used to:

- Track rapid neural dynamics underlying cognitive processes such as attention, memory, and language by analyzing oscillatory brain dynamics.
- Investigate functional connectivity and temporal coordination between brain regions.
- Provide accessible, portable monitoring for patients in intensive care or during sleep studies and coma patients.
- Diagnose and monitor conditions where the margin for temporal error is limited, such as epilepsy, and assessing depth of anesthesia in real time.

In summary, EEG offers various important utilities to clinics and researchers based on its impressive temporal precision, low cost, and portability, making it a powerful tool for real-time brain monitoring even though its source localization is challenged by poor spatial resolution.

3.2 Overview of fMRI

Functional Magnetic Resonance Imaging (fMRI) is a noninvasive neuroimaging technique that measures brain activity indirectly by detecting changes in blood flow. It relies on the Blood-Oxygen-Level-Dependent (BOLD) signal, which reflects changes in the concentration of oxygenated and deoxygenated hemoglobin in the blood in response to neuronal activity in the brain (Bandettini, 2020). Namely, when a specific brain region becomes active, its neurons consume more oxygen, triggering a local increase in blood flow to that area as a response. This hemodynamic response leads to measurable changes in magnetic properties, which can be captured by MRI scanners. However, the BOLD response naturally takes several seconds, which introduces a delay between the neuronal activity and the measured signal. This poor temporal profile makes fMRI less suited for capturing fast neural events.

The main strength of fMRI lies in its ability to localize brain activity with high spatial precision. By recording hemodynamic signals using an MRI scanner instead of electrodes placed on the scalp, fMRI can capture activity within 1 to 3 cubic millimeters, including deep subcortical structures (Huettel et al., 2008). This makes it a powerful tool for exploring the anatomical organization of the brain and mapping networks involved in processes such as memory, emotion, and decision-making.

Despite its limitations, fMRI is essential in cognitive and clinical neuroscience due to its precise spatial resolution. It complements EEG by providing insights into where brain activity occurs, as opposed to when it occurs. As described in Ulmer & Jansen (2020) fMRI is routinely used to:

- Localize brain regions involved in sensory processing, motor execution, language, memory and other cognitive tasks.
- Map the functional anatomy of the brain in healthy individuals and patients.
- Detect spatially localized functional abnormalities in psychiatric conditions.
- Support clinical applications such as presurgical mapping, evaluating treatment efficacy, and pharmacological studies of brain function.

In summary, fMRI provides detailed spatial resolution of brain activity, making it suitable for understanding the functional organization of the brain. Functional organization refers to how different brain regions are specialized for different cognitive processes. Its ability to accurately map active brain regions makes it an indispensable tool in clinical practice and research, especially when combined with EEG to overcome the poor temporal resolution.

3.3 Simultaneous EEG-fMRI Studies

EEG and fMRI both measure neural activity, but they rely on different methods: EEG captures rapid

electrical signals from neuronal populations, while fMRI measures the slower hemodynamic responses associated with neural metabolism. Their simultaneous use gives insights into brain function that neither of these techniques can offer alone. EEG offers temporal resolution able to track electrical signals on a millisecond scale. On the other hand, fMRI has accurate spatial resolution, able to localize neural responses within millimeters across cortical and subcortical structures. Their combination enables researchers to map the "when" from EEG and the "where" from fMRI (Warbrick, 2022).

Simultaneous EEG-fMRI studies have grown steadily over the past 25 years due to their advantages, making significant contributions to cognitive neuroscience, clinical applications, and brain network analysis. However, the promise of combining EEG and fMRI presents various challenges. As simultaneous EEG-fMRI studies record both data in parallel, the EEG cap and the MRI scanner operate at the same time. This introduces many artifacts such as RF-induced heating as a result of conductive EEG components. Furthermore, the EEG cap also interferes with the fMRI recording, producing noise in the data (Chowdhury et al., 2019). As stated in Jorge et al. (2015), the field has made substantial progress, and researchers have introduced practical solutions to these issues. These improvements have established simultaneous EEG-fMRI as a valuable tool in cognitive neuroscience and clinical research.

As such a useful modality, simultaneous EEG-fMRI has been used to discover a variety of cognitive phenomena, including error detection, attention shifts, and conflict processing. Studies have shown that trial-by-trial variations in EEG signals, such as the amplitude of the N2 or P300 response, correspond to changes in the BOLD activation in specific regions such as the anterior cingulate cortex and visual cortex, depending on the task (Eichele et al., 2005; Debener et al., 2005). Additionally, flanker task studies have also demonstrated how specific EEG features align with regional BOLD changes during conflict resolution (Ullsperger & Debener, 2010). This introduces the promise of potentially translating one signal solely based on the other, as some features in EEG appear to predict regional BOLD signal changes.

3.4 EEG Features and fMRI Relevance

The integration of EEG and fMRI begins with EEG-derived features that capture aspects of neural dynamics similarly to the BOLD signal. Even though EEG and fMRI measure brain activity fundamentally differently, there is evidence that suggests certain EEG features correlate with fMRI regional BOLD signal changes. This relationship enables the possible translation between the two modalities. The range of EEG features includes: band power, phase synchronization metrics such as Phase-Locking Value (PLV) and Amplitude Envelope Correlation (AEC), aperiodic 1/f slope, burst dynamics, and global field power (GFP). Event-related potentials (ERPs), while still relevant, are excluded for this study due to the resting state nature of the data used. These features were selected based on their interpretability and prior empirical validation in simultaneous EEG-fMRI studies.

This thesis investigates whether features extracted from EEG data collected during a real-world EEG-fMRI coregistration study can be used to predict patterns typically observed in fMRI signals. While mapping fMRI data onto EEG provides insight into spatial modeling, the opposite approach, predicting fMRI spatial information from EEG data, offers greater practical value. EEG is portable, relatively cheap, and suitable for mobile usage, making it more accessible than fMRI in many real-world settings. Therefore, this thesis focuses on extracting a broad range of features derived from EEG data in order to estimate or translate the EEG signal into an fMRI-like representation with accurate spatial resolution.

3.4.1 Band-Power Metrics

Band power refers to the amplitude of the EEG signal within specific frequency bands; Delta (0.5-4Hz), theta (4-8Hz), alpha (8-13Hz), beta(13-30Hz), and gamma (¿30Hz) each linked to certain cognitive and physiological states. Delta activity typically dominates during deep sleep and slow-wave brain states. Theta is associated with memory encoding, attention, and cognitive control. Alpha power is typically heightened during relaxed wakefulness. Beta activity is related to motor processes, attention, and active problem solving, while

gamma oscillations are linked to conscious perception, working memory, and neural synchronization (Budzynski, 2009).

Various simultaneous EEG-fMRI studies have demonstrated correlations between the oscillatory power in these frequency bands with regional BOLD signal changes. For example, alpha power often shows a negative correlation with BOLD activity in the visual cortex and default mode networks (DMN), while gamma power tends to express a positive correlation with BOLD signals in attention-related regions (Ebrahimzadeh et al., 2022). Furthermore, a review by Wirsich et al. (2018) shows that band power, especially within the alpha and beta ranges, reliably predicts BOLD signal amplitudes across sensory and control networks.

In this thesis, the maximum, minimum, and average amplitude of each frequency band are extracted for each electrode recording. These are marked as features to investigate whether the EEG-derived metrics can accurately predict localized fMRI activity patterns from resting state data.

3.4.2 Peak Frequency

Peak frequency is defined as the dominant frequency across all frequency bands. Even though it is less commonly studied in the context of EEG and fMRI, variations in the individual peak frequency per electrode in EEG have been linked to BOLD responses. A study by Grandy et al. (2013) reveals a significant correlation between individual peak frequency and BOLD signal amplitude increase in the right hemisphere during task-relevant experiments. Furthermore, the study suggests that this individual peak frequency reflects neural dynamics that approximate fMRI networks. In this thesis, peak frequency is explored as a feature possibly capable of predicting individual differences in fMRI signals across cognitive states during resting state data.

3.4.3 Aperiodic 1/f Slope

The aperiodic 1/f slope is a non-oscillatory component of the EEG power spectrum and serves as a measure of the excitation and inhibition balance in cortical networks. This metric is derived by computing the density of the power spectrum and plotting the result on a log-log curve. The 1/f slope is then a line fitted across these points, excluding oscillatory peaks. A flatter slope indicates greater excitation relative to the inhibition in the brain. On the other hand, a steeper slope suggests the opposite (Akbarian et al., 2024).

Because the excitation/inhibition balance influences the overall neural dynamics of the brain, the aperiodic 1/f slope could potentially reflect BOLD signal fluctuations. In this study, the 1/f slope for each epoch and electrode recording across all subjects and sessions is extracted in order to assess whether cortical excitability, measured by the 1/f slope, contributes to predicting spatial patterns shown in fMRI signals.

3.4.4 Burst Dynamics

Burst dynamics are another EEG feature involving short, high amplitude oscillations that occur throughout all frequency bands, most commonly in the beta and gamma range. These bursts reflect brief periods where neuronal activity and synchrony are increased for a short amount of time, which is linked to mental processes such as attention shifts and cognitive transitions also observed in fMRI signals. In clinical EEG literature, amplitude bursts have been observed during normal functioning brains and pathological conditions such as epilepsy or burst-suppression in comatose patients (Sheorajpanday & van Putten, 2006; Tatum, 2015).

These bursts are detected by using a threshold amplitude over short time periods and often shift cortical excitability. A research by Cunningham et al. (2021) analyzed beta-bursts in EEG-fMRI data and demonstrated that these events corresponded to localized increases in BOLD activation in the relevant Regions of Interest (ROIs). This supports a direct link between burst dynamics and hemodynamic responses during cognitive tasks and could still apply during resting state conditions. In this thesis, the burst rate and burst duration are extracted from the EEG data for each electrode recording at each epoch in order to investigate their relation to BOLD signal changes in resting state data to possibly aid in translating the two signals.

3.4.5 Phases Synchronization Metrics: PLV and AEC

Phase synchronization is the temporal coordination of the neural activity between different brain re-

gions. This feature is essential for studying brain dynamics and connects to functional network organization observed in fMRI. Because the BOLD signal reflects synchronized neural activity over time, EEG metrics such as Phase-Locking Value (PLV) and Amplitude-Envelope Correlation (AEC) that capture phase synchronization in EEG are potential predictors of fMRI connectivity patterns.

According to Williams et al. (2023), phase synchronization networks derived from EEG data reveal brain architectures that are anatomically and functionally coherent. This idea proposes that phase synchronization metrics like PLV and AEC can perceive similar brain architectures observed in fMRI networks, only not as accurately. As further evidence, Xi et al. (2022) demonstrated that EEG networks constructed through PLV can reliably differentiate between cognitive states, implying their sensitivity to spatial patterns also observed in fMRI data. Additionally, Chen et al. (2025) used the AEC metric to classify cognitive states, and Zamm et al. (2018) proved during a musical performance study that AEC captures individual synchrony, therefore reinforcing the value of tracking functional connectivity in EEG.

In this thesis, both PLV and AEC are collected for selected electrode pairs to capture functionally relevant brain regions in resting state data. These regions are expected to align with the Default Mode Network (DMN) identified commonly in fMRI studies. The electrode pairs are: F3–F4, C3–C4, O1–O2, T7–T8, Fz–Pz, and P3–P4. These electrode pairs were selected based on their involvement in large-scale brain networks observable in fMRI resting-state data. Prior literature Wirsich et al. (2018) links the connectivity from different electrodes such as the Fz-Pz electrode pair to the DMN activity.

Specifically, PLV captures the consistency of phase differences over time between electrode pairs, indicating the degree of phase synchronization between them. On the other hand, AEC measures the correlation between the amplitude envelopes of oscillatory activity. For slower frequency dynamics, AEC is more relevant as it closely resembles BOLD signal changes. However, both metrics are useful for the study and will be extracted from the EEG data across all electrode pairs selected in order to examine their relationship to resting state fMRI connectivity and assess their potential in predicting spatial patterns shown in fMRI.

3.4.6 Global Field Power (GFP)

Global Field Power (GFP) measures the overall spatial variability of EEG signals across the whole scalp. Specifically, it quantifies the strength of the whole brain's electrical activity and is commonly used to detect instances of increased neural synchronization. GFP provides insight into the whole brain's activity instead of single electrode recordings, and as a predictor, it can be very valuable.

GFP is calculated as the standard deviation of EEG signals across all electrodes at a specific time point, providing simple yet important global information of the brain. In the context of EEG-fMRI translation, GFP serves as a great predictor of global BOLD signal changes, principally in resting state data as large-scale brain dynamics play a bigger role. Clinical EEG studies have grasped the sensitivity of GFP to physiological and pathological states that are also known to influence BOLD patterns observed in fMRI. For example, Yoshimura et al. (2002) demonstrated that GFP can distinguish Alzheimer's disease patients from a control group, a condition that is typically associated with disrupted functional connectivity and reduced BOLD signal coherence in fMRI studies. Additionally, Yamada et al. (2004) found that antipsychotic medication significantly modified GFP levels in healthy individuals, correlating with fMRI findings exhibiting changes in functional connectivity and BOLD fluctuations aligning with antipsychotic treatment.

These findings support the premise that GFP changes, which reflect changes in brain states, could correspond to variability in fMRI signals. In this thesis, GFP will be used as a predictor feature, with each epoch corresponding to a GFP value to identify the overall heightened neural activity and explore the relationship with resting-state BOLD signal changes.

4 Methods

4.1 Dataset

The dataset used in this study consists of a co-registration study with simultaneous EEG and fMRI recordings. It originates from Telesford et al. (2023), and the preprocessing was conducted using the public code repository Nathan Kline Institute (2025). The data were collected from 22

healthy adults between the ages of 23 and 51, using a standard 64-channel EEG cap, and all EEG signals were recorded at a sampling frequency of 5000 Hz. Although multiple experimental conditions were recorded, this thesis focuses only on the resting-state data, which consists of 600-second recordings for each subject and session.

The fMRI recordings, which were acquired simultaneously with the EEG recordings, were obtained using a repetition time (TR) of 1.05 seconds and an echo time (TE) of around 25 milliseconds. These settings make the synchronization with the 5000 Hz EEG valuable for multimodal brain analysis. The data is organized following the BIDS (Brain Imaging Data Structure) format, which is standard for most cases. This ensures consistency across the EEG and fMRI recordings, making the dataset easy to process.

For the EEG data, several preprocessing steps were implemented to create clean signals suitable for analysis. The preprocessing pipeline used was built in EEGLAB and is tailored for simultaneous EEG-fMRI recordings. Firstly, the gradient artifacts which are caused by the MRI scanner were removed using the FMRIB plugin, followed by the detection and correction of cardiac pulse artifacts using the ECG channel. Additionally, downsampling was enforced from the original 5000 Hz to 250 Hz for efficiency, and an exclusion of the ECG and EOG channels. Furthermore, a bandpass filter was applied between 0.3 and 50 Hz in order to focus on relevant brain frequencies and delete noise elements. Very noisy or non-functioning channels were also detected and removed as a part of the preprocessing for EEG, and a method called Artifact Subspace Reconstruction (ASP) was used to clean the remaining bursts of noise in the channels. Finally, the data was re-referenced to the common average, and an independent component analysis (ICA) was performed to identify and delete components reflecting artifacts such as slight muscle activity or eye blinks. The final result after this pipeline is a cleaned EEG dataset ready for analysis.

In parallel, the fMRI data was also preprocessed using a standard BIDS-compliant pipeline based around the Connectome Computation System (CCS). This includes anatomical registration, motion correction, slice-timing correction, nuisance regression, and spatial normalization to MNI space. Additionally, the fMRI data was preprocessed using the Schaefer2018 parcellation; this segments the brain into 100 to 400 functionally different regions of interest (ROIs). For this study, only the 100 parcel separation is used as it aligns better with the EEG data. This parcellation provides a summary of the brain dynamics while also reducing dimensionality, making this dataset tailored to multimodal analysis capable of integrating the high temporal resolution of EEG with the high spatial resolution from fMRI signals.

4.2 EEG Feature Matrix

The input for the translation model consists of EEG data, not in its preprocessed form, but as a matrix of extracted features derived from the preprocessed recordings. The data is segmented into epochs of five seconds each using a sliding window of 1.05 seconds. This approach attempts to minimize data loss, as non-overlapping epochs would exclude a significant amount of information and also increase the amount of data and temporal resolution. A 2.1 second sliding window was also tested, as it aligns with the fMRI TR; however, it was observed that the 1.05 second window was more appropriate as it aligned better with the fMRI time points and data dimensionality. With the use of a MATLAB script, the resulting data is transformed into a matrix where each row corresponds to a specific feature such as the maximum delta amplitude at electrode Fp1, and each row represents one of the 569 epochs in the recording.

The matrix of extracted features includes the maximum, minimum, and average amplitude of each frequency band (delta to gamma) per electrode recording, the aperiodic 1/f slope for each electrode, the burst rate and duration per electrode recording, and the peak frequency of each electrode recording, independent of frequency bands. Additionally, the PLV and AEC are extracted for all the important electrode pairs, and finally the GFP of each epoch.

4.3 Translation Model

The architecture of the model follows a sequence-to-sequence encoder-decoder design using Long Short-Term Memory (LSTM) layers, which are suited for processing time-series data such as EEG and fMRI. The encoder LSTM takes EEG features

as input and encodes them into hidden and cell states. The decoder LSTM then transforms the hidden representation into fMRI activation sequences, generating one time step at a time. A fully connected layer maps each decoder output into activation values for all brain regions.

Both the EEG and fMRI data are first preprocessed before training. All rows from the feature matrix containing missing values (NaNs) are dropped. Each feature was normalized per channel using a z-score normalization to reduce variability across all electrodes and facilitate model training. Specifically, for a feature vector x corresponding to one electrode across epochs, the normalized value x_{Norm} was computed as:

$$x_{\text{Norm}} = \frac{x - \mu_x}{\sigma_x} \tag{4.1}$$

Where μ is the mean and σ is the standard deviation. The time dimension of both the EEG and fMRI is shortened to 184 epochs to align them temporally properly. The model is an encoder LSTM with a single layer per module, a hidden state size of 64 and a dropout is applied to reduce overfitting. L2 weight decay of 1e-4 is used for regularization, and the Adam optimizer with a learning rate of 1e-3 is applied. During training, teacher forcing is introduced with a ratio of 0.5, while the validation and testing sets are performed without teacher forcing to simulate real-world conditions. Early stopping is also applied with a patience of 20 epochs.

The dataset is split into continuous splits: 70% for training, 15% for validation, and 15% for testing. Ensuring that the temporal order of the data is preserved. The model is then trained to minimize the mean squared error (MSE) between the predicted and true fMRI signals. MSE is used for this study as it penalizes differences in signal amplitude.

For each recording, the model training consistently reduced the MSE from around 0.8 to an average of 0.2 over 200 epochs. After training, the model is evaluated on the test split saved, and both the predicted and true fMRI signals are saved for future analysis. The training model weights are also stored for their reuse when evaluating the features.

4.4 Data Validation

To evaluate model performance, multiple metrics are used to quantify prediction accuracy. Primarily, the mean squared error (MSE) is calculated for both the training and testing datasets. MSE is a widely used metric that quantifies the average squared difference between the predicted and true signals at each time point. Squaring the errors prevents positive and negative values from canceling each other out and gives greater weight to large errors. MSE was chosen also because it directly reflects signal amplitude differences, which is very useful for assessing the accuracy of the continuous fMRI predictions. For a predicted fMRI signal y_{pred} and the corresponding ground truth y_{true}, across N regions and T time points, MSE is calculated as:

$$\text{MSE} = \frac{1}{NT} \sum_{i=1}^{N} \sum_{t=1}^{T} \left(y_{\text{true}}[i,t] - y_{\text{pred}}[i,t] \right)^2 \tag{4.2}$$

For the training data, the MSE is recorded across all 200 training epochs, focusing on the best performing epoch and the final epoch. For the testing data, the MSE is calculated only for the selected evaluation epoch. Given the inherent noise in fMRI and EEG data, and the complex nature of these signals, the test MSE is expected to be considerably higher than the training MSE. However, this does not mean the model performance is inadequate, but rather highlights the difficulty and potential nondeterministic nature of the EEG-fMRI translation.

In addition to MSE, the Pearson's correlation coefficient is used to assess the temporal similarity between the predicted and true fMRI signals. This metric is computed for each brain region i across all time points:

$$r_i = \frac{\text{cov}(y_{\text{true}}[i,:], y_{\text{pred}}[i,:])}{\sigma(y_{\text{true}}[i,:])\, \sigma(y_{\text{pred}}[i,:])} \tag{4.3}$$

where cov is the covariance and σ is the standard deviation of the time series for region i. The average correlation across regions summarizes model performance. To complement this, an overall analysis is obtained by flattening the predicted and ground truth matrices into one-dimensional arrays and measuring the correlation over all values:

$$r_{\text{global}} = \frac{\text{cov}(\text{flatten}(y_{\text{true}}), \text{flatten}(y_{\text{pred}}))}{\sigma(\text{flatten}(y_{\text{true}}))\, \sigma(\text{flatten}(y_{\text{pred}}))} \tag{4.4}$$

This provides a global measure of how well the model captures temporal patterns, independent of amplitude differences.

Finally, to investigate the relative predicative power of different EEG feature types, a permutation-based importance test is performed. In this analysis, one specific feature type, such as the 1/f slope or power bands, is removed, and the model is retained to generate predictions. The change in Pearson correlation and MSE is then recorded to investigate the impact of removing that feature type. This analysis aids in interpreting which EEG-derived features are most relevant for predicting fMRI signals. A decrease in correlation suggests the removed feature type is important, while a negligible or negative correlation drop indicates the removed feature is redundant or even interferes with the model's learning.

The translation from EEG to fMRI is a very challenging task, and even optimal models may yield low predictive power due to the complexity and noise of the signals. Furthermore, these modalities may have a non-deterministic relationship, where one cannot simply predict the other.

5 Results

5.1 Quantitative Results

The MSE and Pearson correlation are used to evaluate the performance of the model. Table 5.1 presents the results for a sample of the data, showing the mean Pearson and overall (flattened) value, as well as the training MSE and testing MSE for the first ten recordings. The values for all the recordings can be seen in the appendix. As expected, the training MSE values are generally lower than the testing MSE, reflecting the inherent noise in EEG-fMRI signals and the challenging nature of this translation task. Pearson correlations vary between subjects, with some negative values observed.

5.2 Visualization of the Data

Figure 5.1 presents a time series overlay of the predicted signal and the true signal for subject 19, session 1, region 0. The blue line corresponds to the target output, while the red line indicates the predicted signal. The x-axis shows the time points in the data, and the y-axis is the normalized signal. The plot describes the difference over time between the prediction made by the model and the actual fMRI signal. While this example shows a single region for one subject and session, similar patterns are observed across the dataset. The model generally approaches the temporal dynamics of the fMRI signal, following similar paths of overall increases and decreases, but the actual values of the normalized signal deviate between the ground truth and the predicted signal.

5.3 Feature Contributions

For subject 1, session 1, a permutation-based importance test is applied across all metrics in order to investigate which EEG-derived features contributed most to the prediction of the fMRI signal. Table 5.2 presents the change in Pearson correlation and MSE for each feature type when excluded from the model's input. Positive values indicate removing the feature reduced the predictive power of the model, suggesting the feature is important for the translation. Values near zero or negative values, therefore, indicate minimal contribution or potential interference with accurate predictions. The feature importance analysis shows that band power has the largest impact on model performance, while GFP and the phase synchronization metrics show minimal impact.

6 Discussion

6.1 Interpretation and Implications

6.1.1 Mean Squared Error

As shown in Table 5.1, the training and testing MSE values are presented for the first ten recordings. MSE is a measure of the average squared difference between the predicted values and the ground truth; lower values indicate better predictive accuracy, while values closer to one or higher reflect high deviations from the true values. The training MSE values ranged from 0.16 to 0.24, indicating a good fit to the training data. However, testing MSE values between 0.6 and 1.3 are considerably higher, reflecting a drop in performance on unseen data. This shift between low training and high testing errors suggests overfitting, demonstrating limited generalization, and highlights the difficulty of predicting fMRI signals from EEG features in real-world settings. Despite using techniques like

Table 5.1: Pearson correlations and MSE values for the first 10 recordings.

Subject-Session	Mean Pearson	Overall (flattened) Pearson	Train MSE	Test MSE
sub01-ses1	0.1095	0.1148	0.1638	1.3371
sub02-ses1	0.3540	0.3770	0.2156	0.7241
sub03-ses1	0.2963	0.2967	0.2339	0.9221
sub04-ses1	-0.0280	-0.0003	0.1951	1.2832
sub04-ses2	0.1632	-0.1564	0.1894	1.0326
sub05-ses1	0.3874	0.3681	0.2026	0.8591
sub05-ses2	0.3486	0.3510	0.2375	0.6602
sub06-ses1	0.4131	0.4013	0.2443	0.8629
sub06-ses2	0.2668	0.2503	0.2141	0.8787
sub07-ses1	-0.2486	-0.2548	0.2123	1.2457

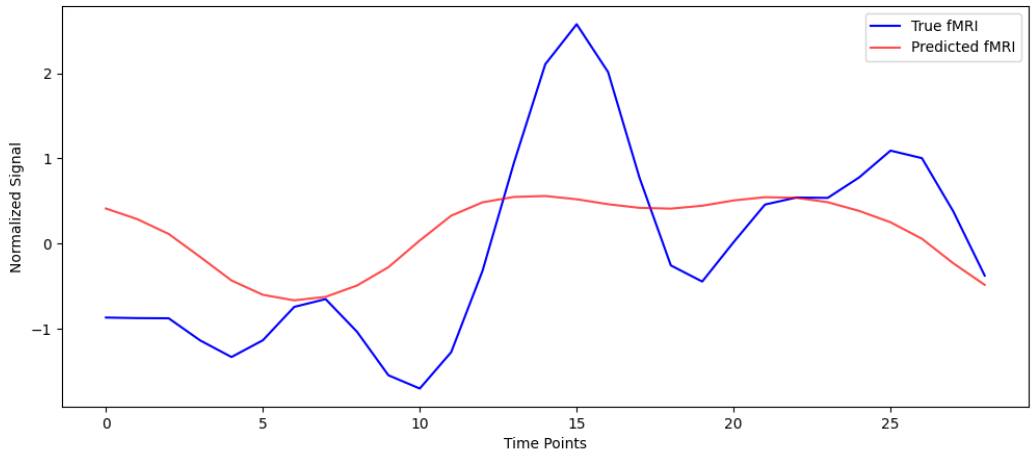

Figure 5.1: Time series overlay of the predicted signal (red) and the true signal (blue) for subject 19 session 1 region 0.

Feature	Change in Pearson's	Change in MSE
Band power	0.1570	0.1744
Aperiodic 1/f slope	0.0414	0.0668
Burst dynamics	0.0253	0.0134
Peak frequency	0.0024	0.0014
AEC	-0.0012	-0.00015
PLV	-0.0021	-0.0032
GFP	-0.0443	-0.0684

Table 5.2: Changes in model performance metrics for different EEG features.

L2 regularization and early stopping to reduce overfitting, these measures were insufficient to achieve strong generalization, likely reflecting the complexity and variability of the EEG and fMRI signals.

6.1.2 Pearson correlation coefficient

The Pearson correlation coefficient, also shown in Table 5.1, presents the mean Pearson and the overall (flattened) Pearson values. For this study, both measures are computed across all epochs of the

data. The mean Pearson represents the average correlation across individual epochs, providing an estimate of how consistently the model performs across the dataset. On the other hand, the overall Pearson flattens all values into one vector of predictions and a corresponding vector of ground truths, then computes a single correlation reflecting how well the model performs on the dataset as a whole. When these values approach one, it indicates a strong positive linear relationship, while values closer to zero suggest a weak or no relationship. Negative values would reflect an inverse relationship. As seen in the table, most values are close to zero or even negative, ranging from 0.4 to -0.25 for both the mean Pearson and the overall Pearson, indicating that the model predictions show only a weak or no relationship to the ground truth. These values are expected since the complexity of the signals and the difficulty of the translation task make it very difficult to achieve accurate predictions.

6.1.3 Permutation-based Importance Test

As shown in Table 5.2, for the first recording from subject 1, session 1, the results from a permutation-based feature importance test are presented. In this method, the model is forced to ignore one feature type and make predictions without it. The change in predictive performance, measured by differences in Pearson correlation and MSE, reflects the relative importance of the excluded feature. A large drop in performance indicates that the feature contributed significantly to accurate predictions, while a minimal change suggests limited predictive value for the specific feature type.

The results show that band power metrics, such as the minimum, maximum, and average amplitudes per frequency band, lead to the largest decrease in predictive accuracy when excluded. This indicates that these features are the most informative for the model. One likely reason is that band power captures fundamental oscillatory activity in a relatively raw form, directly linked to neural dynamics. Furthermore, band power is represented by far more features than any other category, with 885 rows compared to around 60 for the others, which naturally increases its predictive influence.

On the other hand, the aperiodic 1/f slope, peak frequency, and burst dynamics show almost no effect on predictive performance, as the changes in Pearson correlation and MSE are close to zero. The 1/f slope based on prior literature is thought to reflect similar mechanisms then measures in the BOLD signal, but the measure is not simple enough for the model to grasp (Moon et al., 2021). Peak frequency specifically provides limited information per epoch compared to richer feature types such as band power, which likely explains its low importance. Burst dynamics, on the other hand, may be too unpredictable, making it difficult for the model to identify patterns.

Connectivity-related features such as AEC, PLV, and GFP even show negative contributions, meaning that their usage may interfere with predictions instead of improving them. Although measures of phase synchronization are theoretically relevant for EEG to fMRI translation, EEG has limited spatial resolution compared to fMRI, therefore restricting its ability to infer phase synchronization patterns across regions that would otherwise be given by fMRI. This mismatch may explain why these features appear to have negative predictive values in the context of translating EEG to fMRI and would agree with the study conducted by Jiricek et al. (2025).

6.1.4 Graph Interpretation

Figure 5.1 illustrates the difference between the true signal and the predicted signal. This plot highlights that, while the predicted signal partially follows the general trajectory of the true signal, it consistently fails to approximate it with accuracy. The model captures broad patterns, such as the overall increases and decreases in the normalized signal, but it struggles to reproduce detailed information and has various deviations. This lack of generalization reduces the reliability of the predictions, as the results diverge significantly from the target output. Similar behavior was observed across all subject-session pairs and brain regions; even though a slight alignment is seen between the two signals, the model is unable to achieve accurate predictions.

6.2 Limitations

The poor performance from the model in this study is expected, due to the inherent incompatibility between EEG and fMRI signals. However, the results

do suggest that a translation between these two modalities may be possible with further research. It is observed that certain EEG features do contribute to the prediction of fMRI signals slightly, and potentially a more thoroughly trained model could achieve more accurate results. Despite this possibility, various factors limit the accomplishment of this translation. Primarily, the amount of noise present in simultaneous EEG-fMRI recordings becomes problematic even after preprocessing, complicating the learning process of the model and preventing it from learning meaningful patterns and signal relationships. Previous research has shown that simultaneous EEG-fMRI recordings are difficult as the EEG data quality is compromised inside the MRI scanner, with multiple artifacts significantly distorting the signal properties such as the ballistocardiographic (BCG) artifact, even after artifact removal (Gallego-Rudolf et al., 2022). Additionally, the variance in temporal resolution and the difference in data dimensions between the two modalities naturally complicates aligning the signals' time points. While it is theoretically possible to align the signals, it remains a highly complex task. Furthermore, the contrast in spatial resolution present in fMRI and EEG is a fundamental limitation that complicates the translation from EEG to fMRI. As EEG lacks the ability to capture spatial information with the precision of fMRI signals, especially in deep cortical regions, the model has limited spatial information to process an fMRI signal. These limitations highlight the significant challenges of translating these signals; however, the possibility for successful translations is still present with further research and modeling.

6.3 Future Research

In order to achieve a more accurate translation between EEG and fMRI signals, several improvements should be considered for future research. Firstly, using a larger and higher quality simultaneous EEG-fMRI dataset is essential, as the involvement of more subjects, longer recording sessions, and a balance between resting-state and task-based conditions would provide a better foundation for model training. Furthermore, additional recordings such as electrocardiography (ECG) added to the input could also aid the model and remove noise that contaminates both EEG and fMRI recordings. To reduce the inherent spatial mismatch between the two signals, source localization techniques could be applied in order to align the EEG sensory activity onto cortical regions that correspond with the fMRI parcellations. For improvements on the model, future approaches to this translation should provide rigorous feature selection, prioritizing features with high predictive power while ignoring the interfering features. Also, involving the use of hemodynamic response function (HRF) based models in order to account for the natural temporal delay from the BOLD response. An HRF-based model would implement a solution to the temporal mismatch demonstrated by these two modalities and could be integrated into a more advanced architecture. Finally, the implementation of stricter cross-validation and other strategies to reduce overfitting and ensure generalization in order to overcome the current limitations in the model. Collectively, these improvements promise to refine the translation, possibly providing reliable translations between EEG and fMRI.

6.4 Conclusion

This study focuses on investigating the extent to which features derived from EEG signals can be used to predict characteristics typically observed in fMRI signals. Specifically, this thesis explores which EEG metrics such as frequency band power, aperiodic 1/f slope, phase synchrony, burst dynamics, or global field power can predict spatial patterns observed in the BOLD response. The results showed that an accurate translation is not possible with the current model; however, some specific features did appear to slightly predict fMRI signals, and with future investigation, a more appropriate model could potentially be able to produce a successful translation.

This project is significant in its attempt to bridge two modalities that capture different aspects of brain activity. Developing a method able to translate EEG to fMRI signals could improve traditional neuroimaging by complementing the strengths of these techniques without having to conduct both, as fMRI is computationally expensive. The modest predictive value seen from specific EEG features suggests that EEG contains information relevant to fMRI signals, indicating this translation is complicated but theoretically possible.

The results currently highlight the limitations of the translation. As it is shown, the model struggles to generalize past the training set, which indicates the complexity and nonlinearity of the EEG-fMRI relationship. The poor results align with prior research which shows how EEG and fMRI signals have an inherent spatial mismatch, complicating the idea of combining the two modalities (Jiricek et al., 2025). Mediocre results would not suffice for real-world implementation, where inaccurate measures could produce incorrect diagnoses. Although the translation remains theoretically possible, substantial improvements are required before it can be applied in real-world scenarios where accuracy is crucial.

In conclusion, this project demonstrates both the potential and the limitations of translating EEG signals into fMRI-like signals. While the current model still produces unreliable predictions, it is observed how with further investigation, the translation holds promise to create accurate signals. This is seen as some features already do contain predictive value. This study ultimately introduces the idea that achieving an accurate translation between EEG and fMRI could revolutionize neuroimaging and multimodal neuroscience, improving cognitive research and clinical diagnosis, but also introduces the many limitations surrounding this problem.

References

Akbarian, F., Rossi, C., Costers, L., D'hooghe, M. B., D'haeseleer, M., Nagels, G., & Van Schependom, J. (2024). Stimulus-related modulation in the 1/f spectral slope suggests an impaired inhibition during a working memory task in people with multiple sclerosis. *Multiple Sclerosis Journal*, *30*(8), 1036–1046. doi: 10.1177/13524585241239401

Bandettini, P. A. (2020). *fmri.* Cambridge, MA: The MIT Press. Retrieved from `https://www.worldcat.org/oclc/1130310879` doi: 10.7551/mitpress/10584.001.0001

Budzynski, T. H. (2009). *Introduction to Quantitative EEG and Neurofeedback: Advanced Theory and Applications* (2nd ed.). Elsevier & Academic Press.

Chen, J., Wang, Y., Cui, Y., Wang, H., Polat, K., & Alenezi, F. (2025). Eeg-based multi-band functional connectivity using corrected amplitude envelope correlation for identifying unfavorable driving states. *Computer Methods in Biomechanics and Biomedical Engineering*, 1–13.

Chowdhury, M. E. H., Khandakar, A., Mullinger, K. J., Al-Emadi, N., & Bowtell, R. (2019). Simultaneous eeg-fmri: Evaluating the effect of the eeg cap-cabling configuration on the gradient artifact. *Frontiers in Neuroscience*, *13*, 690. doi: 10.3389/fnins.2019.00690

Cunningham, C., et al. (2021). Regional brain correlates of beta bursts in health and psychosis: A concurrent eeg–fmri study. *Biological Psychiatry*. Retrieved from `https://pubmed.ncbi.nlm.nih.gov/33495122/`

Debener, S., Ullsperger, M., Siegel, M., Fiehler, T., Cramon, B. V., & Engel, A. (2005). Trial-by-trial coupling of concurrent electroencephalogram and functional magnetic resonance imaging identifies the dynamics of performance monitoring. *Journal of Neuroscience*, *25*(50), 11730–11737. doi: 10.1523/JNEUROSCI.3286-05.2005

Ebrahimzadeh, E., Saharkhiz, S., Rajabion, L., Baghaei Oskouei, H., Seraji, M., Fayaz, F., ... Soltanian-Zadeh, H. (2022). Simultaneous electroencephalography-functional magnetic resonance imaging for assessment of human brain function. *Frontiers in Systems Neuroscience*, *16*, 934266. doi: 10.3389/fnsys.2022.934266

Eichele, T., Debener, M., Calhoun, Y. S., Kiehl, V., Yurgelun-Todd, T. S., & Makeig, S. (2005). Prediction of human errors by maladaptive changes in event-related brain networks. *Proceedings of the National Academy of Sciences*, *102*(9), 3073–3078. doi: 10.1073/pnas.0409747102

Gallego-Rudolf, J., Corsi-Cabrera, M., Concha, L., Ricardo-Garcell, J., & Pasaye-Alcaraz, E. (2022, Dec). Preservation of eeg spectral power features during simultaneous eeg-*fmri*. *Frontiers in Neuroscience*, *16*. doi: 10.3389/fnins.2022.951321

Grandy, T. H., Werkle-Bergner, M., Chicherio, C., Schmiedek, F., Lövden, M., & Lindenberger, U.

(2013). Peak individual alpha frequency qualifies as a stable neurophysiological trait marker in healthy younger and older adults. *Psychophysiology*, *50*(6), 570–582. Retrieved from https://pubmed.ncbi.nlm.nih.gov/29375349/ doi: 10.1111/psyp.12043

Huettel, S. A., Song, A. W., & McCarthy, G. (2008). *Functional magnetic resonance imaging* (2nd ed.). Sunderland, MA: Sinauer Associates Inc. Retrieved from https://www.worldcat.org/oclc/777396331

Im, C.-H. (2018). *Computational EEG Analysis: Methods and Applications*. Springer. Retrieved from https://doi.org/10.1007/978-981-13-0908-3 doi: 10.1007/978-981-13-0908-3

Jiricek, S., Koudelka, V., Mantini, D., Marecek, R., & Hlinka, J. (2025, 14). Spatial (mis)match between eeg and fmri signal patterns revealed by spatio-spectral source-space eeg decomposition. *Frontiers in Neuroscience*, *19*, 1549172. doi: 10.3389/fnins.2025.1549172

Jorge, J., Grouiller, F., Ipek, , Stoermer, R., Michel, C. M., Figueiredo, P., ... Gruetter, R. (2015). Simultaneous eeg-fmri at ultra-high field: Artifact prevention and safety assessment. *NeuroImage*, *105*, 132–144. Retrieved from https://doi.org/10.1016/j.neuroimage.2014.10.055

Misulis, K. E., & Abou-Khalil, B. (2013). *Atlas of EEG, Seizure Semiology, and Management* (2nd ed.). Oxford University Press. Retrieved from http://site.ebrary.com/id/10775435

Moon, H. S., Jiang, H., Vo, T. T., Jung, W. B., Vazquez, A. L., & Kim, S.-G. (2021). Contribution of excitatory and inhibitory neuronal activity to bold fmri. *NeuroImage*, *245*, 118676. Retrieved from https://pubmed.ncbi.nlm.nih.gov/33895810/

Nathan Kline Institute. (2025). *Natview_eegfmri: Code for preprocessing data for the naturalistic viewing eeg–fmri data release from nki.* https://github.com/NathanKlineInstitute/NATVIEW_EEGFMRI. (GitHub repository)

Sheorajpanday, R., & van Putten, M. (2006). *Atlas of eeg patterns*. Thieme. Retrieved from https://rug.on.worldcat.org/search/detail/873761812

Tatum, W. O. (2015). *Atlas of critical care eeg*. Wiley-Blackwell. Retrieved from https://rug.on.worldcat.org/search/detail/778262043

Telesford, Q. K., Gonzalez-Moreira, E., Xu, T., Tian, Y., Colcombe, S. J., Cloud, J., ... Franco, A. R. (2023). An open-access dataset of naturalistic viewing using simultaneous eeg-fmri. *Scientific Data*, *10*, 554. Retrieved from https://doi.org/10.1038/s41597-023-02458-8 doi: 10.1038/s41597-023-02458-8

Ullsperger, M., & Debener, S. (2010). Simultaneous eeg and fmri: recording, analysis, and application in cognitive research. *Clinical EEG and Neuroscience*, *41*(3), 121–131. doi: 10.1177/155005941004100308

Ulmer, S., & Jansen, O. (Eds.). (2020). *fmri: Basics and clinical applications* (3rd ed.). Cham: Springer. Retrieved from https://www.worldcat.org/oclc/1154534329 doi: 10.1007/978-3-030-41874-8

Warbrick, T. (2022). Simultaneous eeg-fmri: What have we learned and what does the future hold? *Sensors*, *22*(6), 2262. doi: 10.3390/s22062262

Williams, N., Wang, S. H., Arnulfo, G., Nobili, L., Palva, S., & Palva, J. M. (2023). Modules in connectomes of phase-synchronization comprise anatomically contiguous, functionally related regions. *NeuroImage*, *272*.

Wirsich, J., Giraud, A.-L., & Sadaghiani, S. (2018). Concurrent eeg- and fmri-derived functional connectomes exhibit linked dynamics. *bioRxiv*. doi: 10.1101/464438

Xi, J., Huang, X.-L., Dang, X.-Y., Ge, B.-B., Chen, Y., & Ge, Y. (2022). Classification for memory activities: Experiments and eeg analysis based on networks constructed via phase-locking value. *Computational and Mathematical Methods in Medicine*, *2022*.

Yamada, K., Isotani, T., Irisawa, S., Yoshimura, M., Tajika, A., Yagyu, T., ... Kinoshita, T. (2004). Eeg global field power spectrum changes

after a single dose of atypical antipsychotics in healthy volunteers. *Brain Topography*, *16*(4), 281–285.

Yoshimura, M., Zhang, H., Isotani, T., Tamagaki, C., Yoshida, T., Sugiyama, M., ... Kinoshita, T. (2002). Global field power and low resolution electromagnetic tomography solutions in alzheimer's disease. *International Congress Series*, *1232*, 751–755.

Zamm, A., Debener, S., Bauer, A.-K. R., Bleichner, M. G., Demos, A. P., & Palmer, C. (2018). Amplitude envelope correlations measure synchronous cortical oscillations in performing musicians. *Annals of the New York Academy of Sciences*, *1423*(1), 251–263.

A Appendix

Table A.1: Pearson correlation and MSE values.

Subject-Session	Mean Pearson	Overall (flattened) Pearson	Train MSE	Test MSE
sub01-ses1	0.1095	0.1148	0.1638	1.3371
sub02-ses1	0.3540	0.3770	0.2156	0.7241
sub03-ses1	0.2963	0.2967	0.2339	0.9221
sub04-ses1	-0.0280	-0.0003	0.1951	1.2832
sub04-ses2	0.1632	-0.1564	0.1894	1.0326
sub05-ses1	0.3874	0.3681	0.2026	0.8591
sub05-ses2	0.3486	0.3510	0.2375	0.6602
sub06-ses1	0.4131	0.4013	0.2443	0.8629
sub06-ses2	0.2668	0.2503	0.2141	0.8787
sub07-ses1	-0.2486	-0.2548	0.2123	1.2457
sub07-ses2	-0.0240	0.0098	0.7127	1.3485
sub08-ses1	0.6243	0.6093	0.4915	0.6205
sub08-ses2	0.1416	0.0933	0.5777	0.5860
sub09-ses1	0.0868	0.0957	0.7574	0.8294
sub10-ses1	-0.0250	0.0808	0.5491	0.9419
sub10-ses2	0.2770	0.2842	0.6019	0.9879
sub11-ses1	0.0957	0.0962	0.7906	1.2470
sub11-ses2	-0.3130	0.1057	0.6383	0.6248
sub12-ses1	0.1894	0.1463	0.5061	1.2727
sub12-ses2	0.3279	0.3161	0.6391	0.7937
sub13-ses1	0.2429	0.2252	0.4632	0.9780
sub13-ses2	0.2985	0.0869	0.7739	0.9289
sub14-ses1	-0.0689	-0.0648	0.4173	1.4224
sub14-ses2	-0.0360	-0.0099	0.6091	1.0411
sub15-ses1	0.1049	0.0885	0.3931	1.2470
sub15-ses2	0.1636	0.1655	0.5398	0.9208
sub16-ses1	0.4958	0.0964	0.7645	1.1405
sub16-ses2	0.0725	0.1069	0.7988	1.1649
sub17-ses1	0.0296	0.0937	0.6409	1.4125
sub17-ses2	0.3553	0.1055	0.4897	0.8501
sub18-ses1	0.1233	0.0895	0.7083	0.7593
sub19-ses1	0.1154	0.1403	0.5486	1.4394
sub19-ses2	-0.0284	-0.0252	0.4131	1.6254
sub20-ses1	0.0825	0.0736	0.8510	0.7981
sub20-ses2	0.2147	0.1942	0.4180	1.0512
sub21-ses1	-0.1366	0.0824	0.5424	0.6518
sub21-ses2	0.0381	0.1067	0.8499	1.1486
sub22-ses1	0.1277	0.1464	0.5462	0.8018
sub22-ses2	-0.1042	-0.0239	0.6679	1.0459